



Journal Name

ARTICLE

Heterogeneous alkaline earth metal-transition metal bimetallic catalysts for synthesis of biodiesel from low grade unrefined feedstock

Received 00th January 20xx,
Accepted 00th January 20xx

DOI: 10.1039/x0xx00000x

Tsz-Lung Kwong^a and Ka-Fu Yung^{*a}

www.rsc.org/

A bimetallic alkaline earth metal-transition metal oxide synthesized by a method of direct low-temperature decomposition of bimetallic complex was reported for synthesis of biodiesel. Due to the high phase purity of Ca/Fe catalytic system and its catalytic stability and robustness, the Ca/Fe catalyst was selected for further investigation. The conversion could be achieved at 99.5 % in transesterification for 1 h under the optimal conditions: feedstock-to methanol (1 : 20), catalyst loading (6 wt.%) and temperature (120 °C). ANOVA test suggested that the reaction temperature was discerned as the most prominent factor which contributed 82.84 % to overall catalytic feedstock conversion. In addition, the Ca/Fe catalytic system demonstrated a high FFA tolerance of 2 wt.% and water tolerance of 1 wt.% with remarkable catalytic activity in one-step biodiesel synthesis.

1. Introduction

The limiting fossil fuel reserve and the associated environmental pollutions have prompted scientists to search a sustainable liquid fuel for supporting our future needs. Biodiesel is found to be one of promising renewable energy sources because of its non-toxicity, carbon neutrality with low sulphur content and the similar physical and chemical properties compared to conventional diesel fuel. It may abridge the harmful emission such as NO_x, SO_x, CO, CO₂, unburnt hydrocarbon and particulates.¹⁻⁴ The transesterification involves the breaking down of triglyceride with alcohol.^{1, 2, 4} The homogeneous catalyst for the traditional biodiesel synthesis can be divided into two main groups including strong base (e.g. NaOH or KOH) and strong acid (e.g. H₂SO₄ or HCl).^{5, 6} However, large quantity of fresh water is required for final product purification.

The uses of different heterogeneous base catalysts for catalytic transesterification, such as alkaline earth metal oxides and hydroxides, have widely been reported in literature.⁷⁻¹¹ Mootabadi et al.⁶ investigated that the catalytic activities of alkaline earth metal oxides, including magnesium oxide (MgO), calcium oxide (CaO), strontium oxide (SrO) and barium oxide (BaO), were closely related to their surface basic strength. The basicity increased with atomic number, which increased with larger cationic size and lower polarizing power. This

destabilized the O²⁻ anions.¹² As a result, the catalytic activities of the four catalysts showed a sequence of MgO < CaO < SrO < BaO.¹³ BaO is the strongest basic oxide but it is soluble in methanol and exhibits a high toxicity.⁹ Although SrO is insoluble in methanol, it would be deactivated by atmospheric moisture and carbon dioxide (CO₂).¹³

It is believed that CaO is one of the reactive single oxides and has widely been employed for transesterification reaction because of its high catalytic activity and low preparation cost. However, the use of alkaline metal oxides often confronts with low durability and serious leaching problem due to metal dissolution. It accounts for the loss of active species from the metal oxides catalysts so that the catalytic activities decline significantly upon regeneration.¹⁴⁻¹⁶ Furthermore, the adsorption of water molecules and CO₂ on the active sites of the alkaline earth metal oxides would suppress the esterification and transesterification reactions.^{16, 17}

In order to improve the dissolution of the active metal, various alkali metal oxides supported on alumina¹⁸⁻²⁰, CaO support on silica²¹ and CaO mixed with zinc oxide (ZnO)^{22, 23} have been reported as heterogeneous catalysts towards transesterification. However, it was found that the leaching was not improved as these catalysts demonstrated poor reusability and robustness. More recently, synthesis of mixed metal oxides such as hydrotalcites²⁴ and Ca-La mixed oxide has been explored.²⁵ In the previous work, we studied the transesterification of *Camelina Sativa* oil with methanol to synthesize biodiesel using Na_{0.1}Ca_{0.9}TiO₃ nanorods as heterogeneous catalyst, which synthesized by alkali hydrothermal synthesis.²⁶ The leaching was not improved due to the existence of single oxides.¹⁶ Furthermore, low grade alcohols and unrefined feedstock containing high degree of water cause the hydrolysis of triglyceride to form diglyceride

^aDepartment of Applied Biology and Chemical Technology, The Hong Kong Polytechnic University, Hung Hom, Kowloon, Hong Kong. E-mail: bckfyung@polyu.edu.hk; Tel: +852 3400 8863; Fax: +852 2364 9932
Electronic Supplementary Information (ESI) available: See DOI: 10.1039/x0xx00000x

and free fatty acid (FFA) while the high FFA contaminant will subsequently induce saponification and deactivate the base catalysts.^{27, 28}

Owing to the high toxicity of Ba and the low stability of Sr in air, this study focused on Mg and Ca towards biodiesel synthesis from low grade feedstock with high FFA contaminant. The most abundant transition metal, such as iron (Fe), manganese (Mn) and chromium (Cr), was proposed to act as a stabilizer to retain alkaline earth metal, like Mg and Ca, in bimetallic catalytic system and further enhanced its catalytic stability and robustness. Srebrodolskite typed materials is one of the heterogeneous catalysts for various applications. This material with a general formula of $A_2B_2O_5$ consists of divalent cations and trivalent cations. The conventional synthesis of srebrodolskite $Ca_2Fe_2O_5$ involves the mixing and grinding of CaO and Fe_2O_3 followed by a high temperature calcination at over 1000 °C for 3 h in air.²⁹ These harsh synthetic conditions would surely lead to the formation of highly aggregated particles which decrease the resultant surface area-to-volume ratio. Co-precipitation is another commonly employed preparation method which induces phase separation of metal oxide instead of forming a single phase mixed metal oxide finally. Xue and co-workers has been reported that the synthesis of $Ca_2Fe_2O_4$ - $Ca_2Fe_2O_5$ -based catalyst for biodiesel synthesis, however, a mixed phased of catalyst was observed.³⁰

Herein, a series of alkaline earth metal-transition metal bimetallic oxide catalysts towards transesterification with methanol has been investigated. These mixed oxide catalysts have been synthesized by low-temperature decomposition of the corresponding bimetallic complex in which the bimetallic complex is directly calcinated in atmospheric condition to yield the desired catalyst. The switching of the inorganic metal salts to organometallic complexes is found to significantly decrease the calcination temperature which prevents the formation of highly aggregated catalyst. The FFA and water tolerance of the catalytic system were also investigated. Meanwhile, the reaction conditions for transesterification were optimized. The optimization is very important to maximize the biodiesel yield and to minimize the production cost. Stepwise approach has been extensively employed, however, it is relatively time consuming and difficult to determine the optimal conditions as some of the reaction conditions simultaneous affect the biodiesel yield. Taguchi analysis is a cost effective and time saving alternative approach for optimization in which the analysis can be divided into orthogonal array experiment, signal-to-noise (S/N) ratio analysis and range analysis.³¹⁻³⁵ Analysis of variance (ANOVA) was also introduced as a statistical model to evaluate whether the factors were prominent by F-test under consideration of experimental error.

2. Materials and Method

2.1. Materials

Refined food grade canola oil was obtained from local store in Hong Kong. Crude rice bran oil was obtained from local store

in China. Crude flaxseed and rapeseed oil were produced from an in-house cold-pressed oil extractor using flaxseed and rapeseed obtained from local store in Hong Kong. Waste cooking oil was collected from local restaurant in Hong Kong. Calcium nitrate tetrahydrate ($Ca(NO_3)_2 \cdot 4H_2O$, 99 %) was purchased in laboratory reagent grade from BDH Chemical Ltd. Iron(III) nitrate nonahydrate ($Fe(NO_3)_3 \cdot 9H_2O$, >99 %), magnesium nitrate hexahydrate ($Mg(NO_3)_2 \cdot 6H_2O$, 99 %) and manganese(II) nitrate tetrahydrate ($Mn(NO_3)_2 \cdot 4H_2O$) were supplied by Acros. Ethylenediaminetetraacetic acid (EDTA, 99 %) was obtained from Research Chemical Limited. Chromium(III) nitrate nonahydrate ($Cr(NO_3)_3 \cdot 9H_2O$, 99 %), polyvinylpyrrolidone (PVP, average M_w 40000), methyl yellow, neutral red, bromothymol blue, phenolphthalein, nile blue, tropaeolin O and 2,4-dinitraniline were collected from Sigma Aldrich. Oleic acid ($C_{18}H_{34}O_2$, 99.9 %) was obtained in laboratory reagent grade from Fisher Chemical. Methanol (CH_3OH , 99.8 %) and diethyl ether ($C_4H_{10}O$, 99.5 %) were obtained as ACS reagent grade. Aqueous ammonia solution (NH_4OH , 28.0 – 30.0 wt.%) and potassium hydroxide (KOH) were purchased from UNI-CHEM.

2.2. Catalytic preparation and characterization

2.2.1. Catalyst preparation. Mixed oxides were synthesized by a simple direct decomposition of its corresponding bimetallic metal complex. Ethylenediaminetetraacetic acid (EDTA, 1 mol) was dissolved in milli-Q water followed by adding four equivalence of ammonia water (4 mol). Aqueous polyvinylpyrrolidone solution was added into the ammonium EDTA solution in a drop-wise manner. The solution was stand for stirring vigorously at 60 °C for 15 min. The mixed metal solution (1 :1 mol/mol, 10 mL) was prepared in milli-Q water and was added drop-wisely into reaction mixture. The solution was stirred for further 30 min and finally was dried at 110 °C for overnight. The dried mixed metal EDTA complex precursor was calcinated at 600 °C for 5 h in air.

2.2.2. Catalytic characterization. The size and morphology of the catalyst was characterized by a Hitachi S-4800 field emission scanning electron microscope (SEM, 5 kV) equipped with energy dispersive spectrometry (EDX) with Horiba EMAX EDS detectors. Powder X-ray diffraction (XRD) pattern was obtained by a Rigaku SmartLab X-ray Diffractometer using a $CuK\alpha$ ($\lambda = 1.54056$, 45 kV, 200 mA) radiation with 2θ ranged from 10° to 80° with a step size of 0.02° in scan rate of 5° min⁻¹. Hammett indicator analysis was applied to elucidate the surface basic strength of the catalyst. The catalyst (5 mg) was immersed in methanolic Hammett indicator solution (1 mL, 50 μ M) under ultrasonic irradiation and was allowed to stand for 1 h to achieve equilibrium. The Hammett indicators used for analysis were methyl yellow ($H_- = 3.3$), neutral red ($H_- = 6.8$), bromothymol blue ($H_- = 7.2$) and phenolphthalein ($H_- = 9.7$), nile blue ($H_- = 10.2$), tropaeolin O ($H_- = 11.0$) and 2,4-dinitraniline ($H_- = 15.0$). The surface area analysis was performed using a Quantachrome Autosorb iQ gas sorption analyzer. The sample was outgassed at 0.03 torr with a 2 °C

min⁻¹ ramp to 130 °C and held at 130 °C for 20 h. The sample was then held at vacuum until the analysis was performed using N₂ at 77K (P/P₀ range 1 x10⁻⁵ to 0.995).

2.3. Feedstock evaluation

With referenced to ASTM D664, a standard titration method with a titrant of standard KOH solution was applied in determination of the acidity (AD) and acid value (AV) for all feedstock while the quantity of water was estimated by Karl Fischer titration based on ASTM D4377 using an automated V20 Volumetric Karl-Fischer Titrator. The AD and AV of various feedstock are ranged from 0.11 to 2.00 wt.% and from 0.22 to 3.98 mg_{KOH}/g respectively as summarized in Table 1.

Fatty acid profile of each feedstock was analyzed on a HEWLETT 5890 SERIES II Gas Chromatograph system equipped with a flame-ionization detector and a capillary column (DURABOND-WAX, 30 m x 0.250 mm, film thickness 0.5 μm, Part No.: 122-7033). The operating conditions for the analysis

were as below: injector temperature was 280 °C; detector temperature was 280 °C; temperature program was started at 180 °C in a rate of 2 °C/min to 240 °C. All feedstock are containing fatty acid chain length of 16 to 22 which are desirable for biodiesel synthesis as summarized in supplementary section (Table 2).

Table 1 Acidity, acid value and water content for each feedstock sample

Feedstock	AD (wt.%)	AV (mg _{KOH} /g)	Water (wt.%)
Refined food grade canola oil	0.11	0.22	0.13
Crude flaxseed oil	1.16	2.32	0.12
Crude rapeseed oil	1.65	3.28	0.13
Crude rice bran oil	2.00	3.98	0.11
Waste cooking oil	0.65	1.29	0.12

Table 2 Fatty acid composition for each feedstock sample

Feedstock	Fatty acid composition ^a (%)						
	C _{16:0}	C _{18:0}	C _{18:1}	C _{18:2}	C _{18:3}	C _{20:1}	C _{22:1}
Refined food grade canola oil	5.00	2.68	63.06	22.82	6.44	–	–
Crude flaxseed oil	6.06	2.53	19.19	24.34	47.88	–	–
Crude rapeseed oil	3.91	1.41	17.05	12.94	9.03	14.54	41.12
Crude rice bran oil	19.33	2.79	43.66	34.22	–	–	–
Waste cooking oil	21.88	5.15	56.73	14.48	0.86	0.90	–

^a C_{16:0} = palmitic acid, C_{18:0} = stearic acid, C_{18:1} = oleic acid, C_{18:2} = linoleic acid, C_{18:3} = linolenic acid, C_{20:1} = eicosenoic acid and C_{22:1} = erucic acid.

2.4. Catalytic study

All catalytic reactions were conducted in a stirred batch reactor containing methanol, catalyst and feedstock sample (0.46 g) with different ratio as specified in the detailed results and discussion part. The reaction mixture was heated with a constant vigorous stirring at 750 rpm at a specific temperature for predesigned time. The reaction mixture was separated from the catalyst when the reaction was completed. The feedstock conversion was determined using ¹H-NMR spectroscopy (Bruker, 400 MHz) with CDCl₃. The feedstock conversion was calculated according to the integral ratio of the signal of the -OCH₃ in methyl ester over that of the α-CH₂ in triglyceride and methyl ester as follow,³⁶⁻³⁹

$$\text{conversion (\%)} = \frac{I_{\text{-OCH}_3/3}}{I_{\alpha\text{-CH}_2/2}} \times 100\% \quad (1)$$

The reaction was allowed to cool down to room temperature after completion of the catalytic reaction. The used catalyst was isolated out and was dried at room temperature for the next cycle of catalytic reaction without any washing steps. The same amount of fresh feedstock and methanol were added to the recycled catalyst and the catalytic study was performed for several cycles under the same conditions.

The quantity of active metals leached to the biodiesel layer from the catalyst was determined using inductively coupled plasma optical emission spectroscopy (ICP-OES) by Agilent Technologies 700 Series ICP-OES. A sample of 0.1 mL was pre-digested in a mixture of concentrated hydrochloric acid and concentrated nitric acid (3 : 1 v/v) at a temperature of 60 °C for 2 h.

3. Results and discussion

3.1 Characterization of mixed oxide catalysts

The morphologies of all catalytic systems were characterized by SEM as shown in Fig. 1. The Mg/Fe and Ca/Fe catalytic systems are found to be adopting a nanoparticle. TEM micrograph of Ca/Fe catalytic system also shows nanoparticle morphology with average particle size of 110.8 ± 3.5 nm. Other catalytic systems, however, are exhibiting irregular nanoparticles with different sizes. The EDX analysis was performed to determine the elemental composition and their corresponding ratio of six catalytic systems. The results are tabulated in Table 3. It is found that all six catalytic systems are found to be nearly 1.

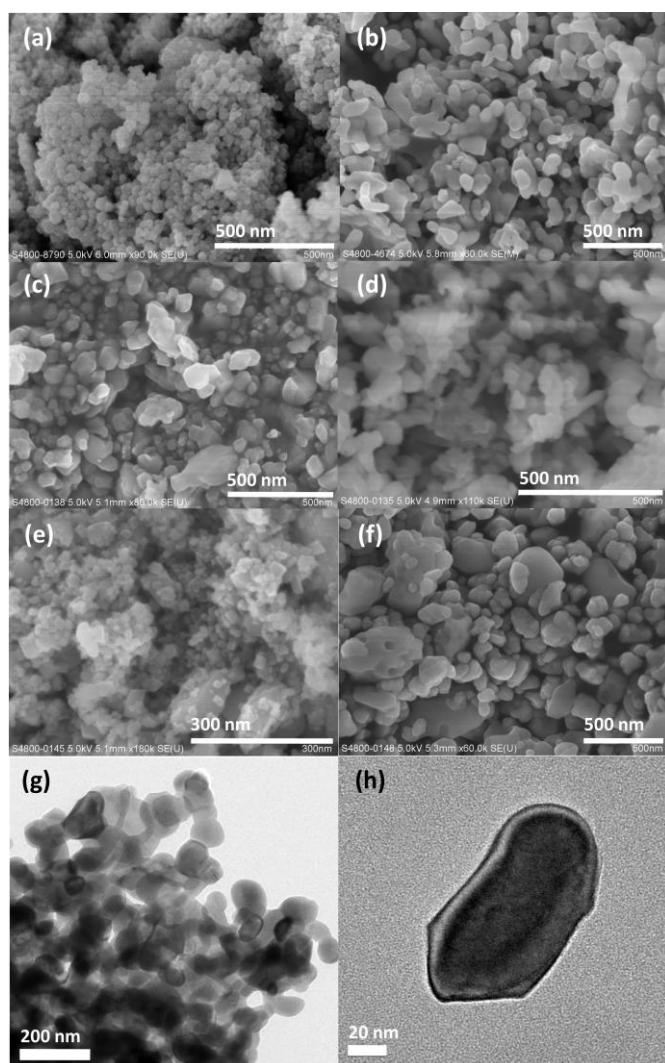


Fig. 1. SEM micrograph of (a) Mg/Fe, (b) Ca/Fe, (c) Mg/Mn, (d) Ca/Mn, (e) Mg/Cr and (f) Ca/Cr catalytic system. (g) TEM and (h) HR-TEM of Ca/Fe nanoparticle.

The crystal structures of the all catalysts were characterized by XRD as depicted in Fig. 2. High phase purity of XRD pattern is observed for Ca/Fe which match to orthorhombic phased $\text{Ca}_2\text{Fe}_2\text{O}_5$ (ICDD: 01-076-8615) respectively. For Mg/Fe catalytic system, it is suspected that the amorphous MgO is present as only cubic phased MgFe_2O_4 (ICDD: 01-088-1936) was found in XRD analysis with a theoretical Mg-to-Fe ratio of 0.5 which deviated from atomic ratio found in the EDX analysis. Mixed XRD patterns obtained in Mg/Mn catalytic system are attributed to tetragonal phased MgMn_2O_4 (ICDD: 01-074-2023), hexagonal phased MgMnO_3 (ICDD: 024-0736) and single orthorhombic Mn_3O_4 (ICDD: 01-072-7943). The diffraction peaks in Ca/Mn catalytic system show agreement to mixed phase of orthorhombic CaMn_2O_4 (ICDD: 01-072-6399) and monoclinic $\text{Ca}_2\text{Mn}_3\text{O}_8$ (ICDD: 034-0469). Both XRD pattern of

Mg/Cr and Ca/Cr catalytic systems demonstrate cubic MgCr_2O_4 (ICDD: 010-0351) and tetragonal CaCrO_4 (ICDD: 008-0458) respectively, however, single Cr_2O_3 is found in both catalytic systems. Single phase mixed oxide is obtained only in Mg/Fe and Ca/Fe catalytic system due to well-matched of Mg(II) ion or Ca(II) ion to Fe(III) ion. In contrast, mix phase of mixed metal oxides are observed in other catalytic systems, probably due to the size mismatched of alkaline earth metal ion and transition metal ion. It is well known that both Mn and Cr have multiple stable oxidation states. Under atmospheric condition at 600 °C, Mn^{3+} and Cr^{3+} should be oxidized to higher oxidation state. Therefore, a mixture of single oxide and mixed oxide was obtained for Mn or Cr containing catalytic systems as suggested by XRD analysis.

Table 3 Characterization and the catalytic performance of a series of catalysts

Catalytic system	Atomic ratio in EDX analysis	Surface basicity
Mg/Fe	1.1	$7.2 < H_- < 9.7$
Ca/Fe	1.0	$10.2 < H_- < 11.0$
Mg/Mn	1.0	$7.2 < H_- < 9.7$
Ca/Mn	0.9	$9.7 < H_- < 10.2$
Mg/Cr	0.9	$7.2 < H_- < 9.7$
Ca/Cr	0.9	$7.2 < H_- < 9.7$
CaO	–	$10.2 < H_- < 11.0$

It has been reported that the basic sites on the surface of heterogeneous catalyst are the active sites for the catalytic transesterification.^{40, 41} Therefore, it is important to investigate the correlation between the surface basic strength and the catalytic activity of the heterogeneous catalyst. As shown in Table 3, all catalytic systems demonstrate a basic property on the catalyst surface as detected by Hammett indicator analysis. The Ca/Fe catalytic system and single CaO exhibit the highest surface basicity with $10.2 < H_- < 11.0$, which could be considered as strong solid bases while the Ca/Mn catalytic system was considered as mild solid base catalyst with $9.7 < H_- < 10.2$. The Mg/Fe, Mg/Mn, Mg/Cr and Ca/Cr catalytic systems were considered as neutral to weak basic catalyst with low surface basicity of $7.2 < H_- < 9.7$. The surface basicity of Ca/Fe catalytic system is much higher than that of the $\text{Ca}_2\text{Fe}_2\text{O}_5$ synthesized through high temperature calcination by Kawashima which is only in range of 7.2 to 9.3.⁴² Other catalytic systems, such as M/Fe, Mg/Mn, Mg/Cr and Ca/Cr, gave relatively low surface basicity in range of 7.2 to 9.7.

The BET specific surface area of Ca/Fe catalytic system was found to be 32.7 m^2/g , as determined from the BET adsorption/desorption isotherm, which is 46 times and 4 times of the surface area reported by Kawashima⁴² and Xue³⁰ respectively.

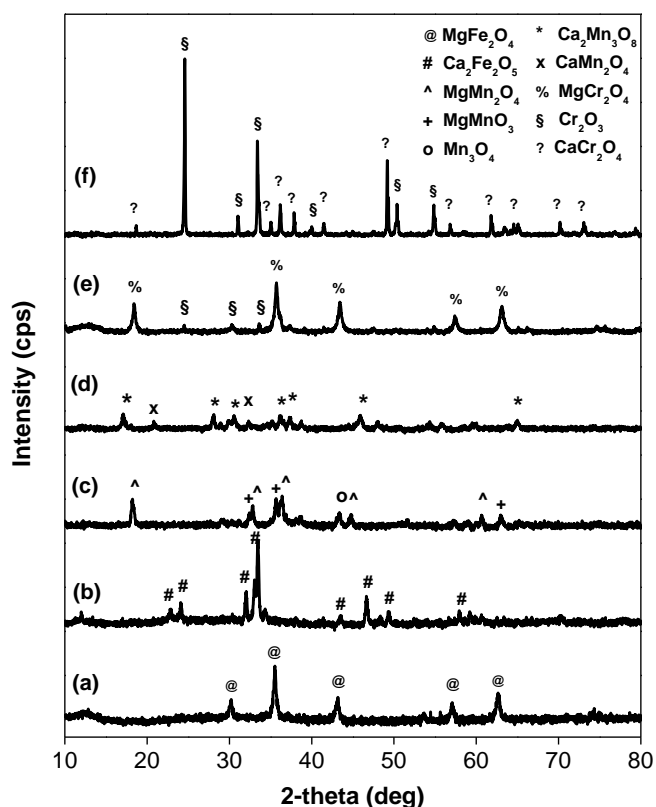


Fig. 2. XRD spectra of (a) Mg/Fe, (b) Ca/Fe, (c) Mg/Mn, (d) Ca/Mn, (e) Mg/Cr and (f) Ca/Cr catalytic system.

3.2 Catalytic activities

The catalytic performances of all catalytic systems were investigated towards transesterification of refined food grade canola oil with the results shown in Table 4. It can be observed that the catalytic activities demonstrated a positive correlation with the surface basicity. Both Ca/Fe and CaO catalytic systems having higher surface basicity gave faster reaction kinetics with conversions of 98.7 % and 99.6 % in 1 hour respectively. The Ca/Mn catalytic system showed a slower kinetics with 97.9 % in 4 h due to the lower surface basicity. Other catalytic systems, however, still gave moderate catalytic conversion due to relatively low surface basicity. The Ca/Fe catalytic system provided higher reaction temperature but in significant shorter reaction time for biodiesel synthesis as compared to the literature reported by Zhang.⁴³ Furthermore, a simple approach of direct reuse of catalyst without further washing steps for used catalyst was employed to investigate the reusability of the catalytic systems.

The Ca/Fe catalyst was the only catalytic system can be reused for over 4 cycles. It demonstrates that the most abundant Fe in bimetallic $\text{Ca}_2\text{Fe}_2\text{O}_5$ catalytic system stabilizes Ca and further enhances its catalytic stability and robustness. In contrast, CaO was completely dissolved at the end of the first cycle which implied that CaO underwent a homogeneous catalysis rather than heterogeneous catalysis and cannot be regenerated for the next cycle.

Table 4 Catalytic performance of mixed oxide catalysts

Catalytic system	Reaction time (h)	Catalytic conversion ^a (%)				
		1	2	3	4	5
Mg/Fe	4	47.3	37.8	25.3	–	–
Ca/Fe	1	98.7	89.0	81.9	71.7	37.5
Mg/Mn	4	71.1	33.9	–	–	–
Ca/Mn	4	97.8	32.4	–	–	–
Mg/Cr	4	79.1	12.9	–	–	–
Ca/Cr	4	80.3	12.5	–	–	–
CaO	1	99.6	–	–	–	–

^a Reaction conditions: feedstock-to-methanol molar ratio (1 : 20), catalyst loading (6 wt.%) and reaction temperature (120 °C).

The EDX analysis of used Ca/Fe catalytic system suggests that the atomic Ca-to-Fe ratio equals to 0.69 which indicates a significant loss of Ca after the fifth cycle catalysis. In order to further confirm the loss of Ca and Fe from the catalyst, amounts of metal leaching was analyzed by ICP-OES on the reaction mixture. As depicted in Table 5, the amount of Ca and Fe leached to biodiesel layer is ranged from 310.5 to 1489.5 mg L^{-1} and 26.9 to 532.7 mg L^{-1} which aligns with the decrease in Ca as suggested in the EDX analysis. It is found that the extent of Ca leached from the bimetallic Ca/Fe system was smaller than that from $\text{CaO}^{14, 15}$ as it was totally dissolved during the catalysis.

Apart from the extension of the catalytic activity, magnetic recycling of used Ca/Fe catalysts was also studied. After ultrasonic treatment of reaction mixture, a strong rare earth based magnet was allowed to place on the side wall of the reaction flask for 30 min, the Ca/Fe catalyst diffused to one side with a strong magnet (see supplementary section Fig. S1). It concludes that the Ca/Fe catalytic system is a magnetic catalyst which favours for magnetic separation and recovery for the next catalytic cycle. Similar observation was observed as reported by Zhang.⁴³

Table 5 Leaching study of Ca/Fe catalytic system for each cycle of transesterification

Cycle	Concentration of metal found in biodiesel layer (mg L^{-1})	
	Ca	Fe
1	1489.5 ± 0.3	532.7 ± 0.3
2	299.8 ± 0.5	114.9 ± 0.3
3	310.5 ± 0.5	80.3 ± 0.2
4	320.3 ± 0.7	112.1 ± 0.3
5	360.2 ± 0.7	26.9 ± 0.2

3.3 Optimization for $\text{Ca}_2\text{Fe}_2\text{O}_5$ catalyzed biodiesel synthesis

Since the $\text{Ca}_2\text{Fe}_2\text{O}_5$ catalytic system gave an excellent robustness towards biodiesel synthesis, its reaction conditions, including feedstock-to-methanol molar ratio (factor A), catalyst loading (factor B) and reaction temperature (factor C), were

then optimized by Taguchi analysis and ANOVA (see supplementary Table S1). Detailed calculations are according to the literature reported by Wu.³³ As tabulated in Table 6, the average feedstock conversion and signal-to-noise (S/N) ratios are ranged from 2.2 % to 78.0 % and from 6.71 to 37.84 respectively. The optimal conditions for each factor as shown in Fig. 3 is clearly distinguished in a combination of $A_2B_3C_3$ as follow: feedstock-to-methanol molar ratio is 1 : 20 (26.5), catalyst loading is 6 wt.% (27.3) and the reaction temperature is 120 °C (33.5). The reaction temperature (factor C) gives the largest range value which indicates that the change of feedstock conversion significantly with the change of the reaction temperature. The $Ca_2Fe_2O_5$ catalyzed transesterification under the optimal reaction conditions as shown in supplementary section (Fig. S2) suggested that a remarkable conversion was achieved at 99.5 % after 1 h and this catalytic system is significant as no observable conversion was obtained in the background reaction.

An increase of the feedstock-to-methanol molar ratio from 1 : 10 to 1 : 30, the feedstock conversion steadily increases and then slightly decreases beyond the optimal ratio (1 : 20). As the transesterification reaction involves three successive reversible reactions, a higher feedstock-to-methanol molar ratio is usually employed to drive the equilibrium to the product side. Other ratios beyond the optimal (1 : 20) does not increase the biodiesel yield as large amount of methanol decreases the concentration of substrate in the reaction mixture.⁴⁴⁻⁴⁶ It is clear that the increase of catalytic conversion with an increase of catalyst loading from 2 wt.% to 6 wt.%. It may due to the availability of more active sites on the catalyst surface to generate alkoxide anions and enhance the catalytic transesterification.^{46, 47} Further increasing in the catalyst loading (6 wt.%) did not enhance the catalytic conversion significantly as amount of active sites were already saturated. Also, it is likely due to the mass transfer inefficiency of catalyst

in three separated phase system and the blockage of active sites by methyl ester products.^{48, 49} The feedstock conversion is found to be enhanced with the reaction temperature increased from 80 °C to 120 °C. The increase in temperature at 120 °C would increase the kinetic energy of substrates which leads to a higher diffusion rate and increase the collision between the $Ca_2Fe_2O_5$ catalyst and the substrates for faster catalytic transesterification.⁵⁰ Furthermore, higher temperature would reduce viscosity of feedstock sample.⁵¹

At the 90 % confidence level, the ANOVA results (Table 7) tabulates $F_A (5.65) < F_B (13.90) > F_C (99.20) > F_A$. The catalyst loading (factor B) and reaction temperature (factor C) are prominent factors affecting the biodiesel yield. Furthermore, the reaction temperature (factor C) gives the highest percent contribution of 82.84 % to the final catalytic activity followed by catalyst loading (factor B, 11.61 %) and feedstock-to-methanol molar ratio (factor A, 4.72 %). The experimental error contributes to 0.83 % which implies that the all experimental results collected in this optimization process are reliable and no important factor is needed to omit.

Kawashima et al.⁴² has reported the preparation of $Ca_2Fe_2O_5$ by the conventional solid-state reaction involving mixing metal oxides as catalyst for transesterification at methanol refluxing temperature with 92 % yield. Xue and co-workers has also reported the synthesis of $Ca_2Fe_2O_4$ - $Ca_2Fe_2O_5$ based catalyst by co-precipitation for biodiesel synthesis with 85.4 % conversion obtained.³⁰ However, the high biodiesel yield obtained under mild conditions is probably due to the presence of single CaO and $CaCO_3$ respectively. In comparison, this novel preparation of high phase purity mesoporous $Ca_2Fe_2O_5$ catalytic system by the direct decomposition of bimetallic Ca/Fe EDTA complex does minimize the formation of unwanted single oxides and carbonates and can still catalyze transesterification with faster kinetics at 120 °C.

Table 6 Orthogonal array experimental design in OA_9 matrix

Entry	Factor			Conversion (%)			Average Y_i (%)	Standard deviation	S/N ratio
	Feedstock : MeOH molar ratio A	Catalyst loading B (wt.%)	Reaction temperature C (°C)	y_1	y_2	y_3			
1	1 : 10	2	80	2.2	2.2	2.1	2.2	0.06	6.71
2	1 : 10	4	100	20.4	20.9	21.1	20.8	0.36	26.36
3	1 : 10	6	120	40.5	40.7	41.4	40.9	0.47	32.23
4	1 : 20	2	100	14.8	14.1	14.6	14.5	0.36	23.22
5	1 : 20	4	120	77.4	78.4	78.2	78.0	0.53	37.84
6	1 : 20	6	80	8.4	8.3	8.0	8.2	0.21	18.31
7	1 : 30	2	120	33.9	33.0	32.8	33.2	0.59	30.43
8	1 : 30	4	80	5.6	5.3	5.3	5.4	0.17	14.64
9	1 : 30	6	100	37.5	36.5	36.0	36.7	0.76	31.28

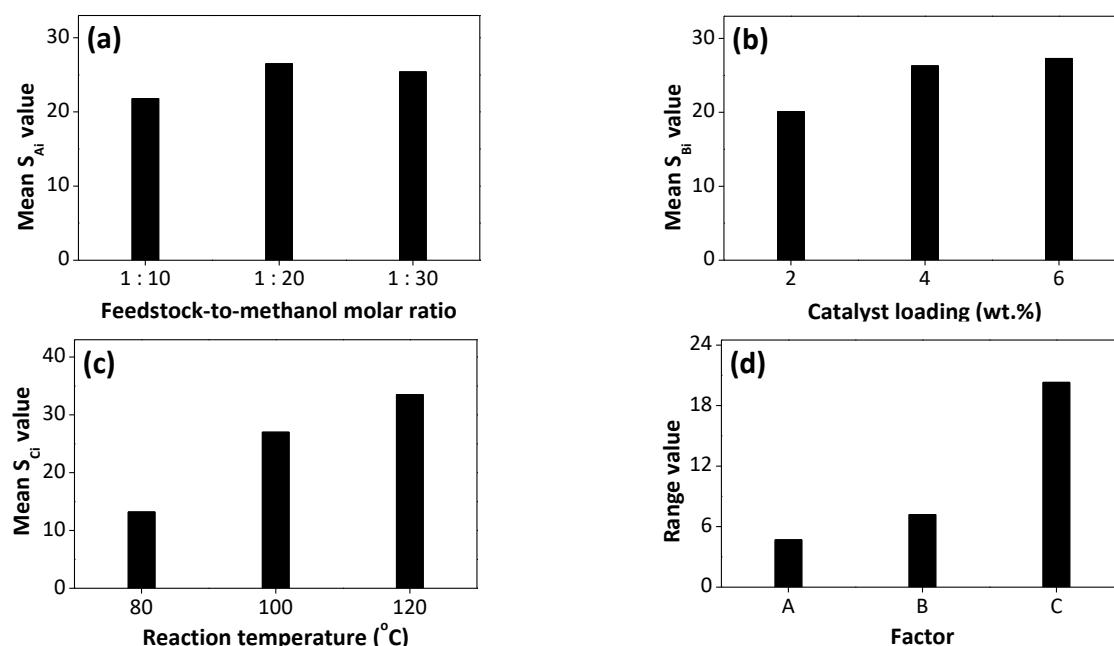


Fig. 3. Relationship between (a) feedstock-to-methanol molar ratio, (b) catalyst loading, (c) reaction temperature and their corresponding mean S_{ji} value. (d) Range values of each factor.

Table 7 Results of ANOVA

Factor	SS_j	dF_j	V_j	F_j	$F_{0.1(2,2)} = 9.00$	P_j (%)
A	36.60	2	18.30	5.65	<	4.72
B	90.06	2	45.03	13.90	>	11.61
C	642.81	2	321.41	99.20	>	82.84
Error	6.47	2	3.24	–	–	0.83
T	775.94	8	–	–	–	100.00

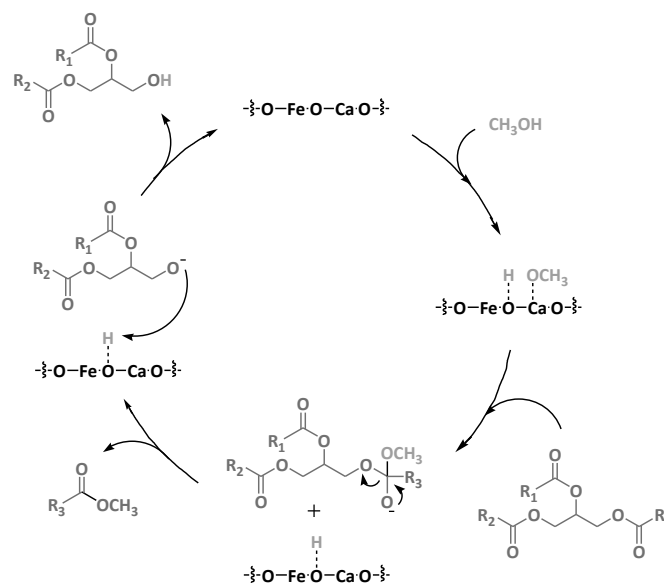
3.4 Effect of reaction temperature and the reaction kinetics

Further investigation was studied on the reaction kinetics of Ca/Fe system catalyzed transesterification. The reaction temperature is found to be the most significant factor in range analysis, which affects the rate of reaction and the feedstock conversion as the intrinsic rate constant is a strongly temperature-dependent function. Due to the excess of methanol, the overall reaction is most likely followed a pseudo-first-order reaction kinetic model. The related equations and the calculation are proposed by literature^{52, 53} can be found in supplementary section. The activation energy (E_a) for the Ca/Fe catalytic system catalyzed transesterification is found to be $45.52 \text{ kJ mol}^{-1}$.

3.5 Proposed mechanism of Ca/Fe catalyzed transesterification

The proposed mechanism of transesterification catalyzed by Ca/Fe catalytic system is proposed in Scheme 1. The transesterification reaction takes place on the surface of the Ca/Fe catalytic system. The first step of the mechanism, O^{2-} on the surface extracts H^+ from methanol molecule to generate methoxide anion which would then nucleophilic attack to the carbonyl carbon of triglyceride molecule to form a tetrahedral intermediate. Subsequently, the rearrangement of tetrahedral

intermediate yields the biodiesel product and diglyceride anion. In the last step, H^+ on the catalyst surface attack the diglyceride anion with regeneration of Ca/Fe catalyst.



Scheme 1. Proposed mechanism of Ca/Fe catalytic system catalyzed transesterification.

3.6 Study of FFA tolerance

Low grade alcohols and unrefined feedstock often possesses a significant amount of water and FFAs which leads to hydrolysis and saponification. Most of the heterogeneous catalysts are active only when the FFAs is significantly removed in pre-treatment process. Therefore, a design and modification of solid catalyst applied to one-step simultaneous esterification and transesterification is gaining more and more concern⁵⁴⁻⁵⁶. The $\text{Ca}_2\text{Fe}_2\text{O}_5$ catalyzed transesterification from various refined and unrefined feedstock serve as a replacement to refined plant oil. As summarized in Table 8, the $\text{Ca}_2\text{Fe}_2\text{O}_5$ catalytic system was performed well in mediocre FFA contaminated feedstock.

Table 8 The $\text{Ca}_2\text{Fe}_2\text{O}_5$ catalyzed biodiesel synthesis with different refined and unrefined feedstock

Entry	Feedstock	Conversion ^a (%)
1	Refined food grade canola oil	98.7
2	Crude flaxseed oil	96.6
3	Crude rapeseed oil	94.8
4	Crude rice bran oil	92.6
5	Waste cooking oil	97.2

^a Reaction conditions: feedstock-to-methanol molar ratio (1 : 20), catalyst loading (6 wt.%), reaction temperature (120 °C) and reaction time (1 h).

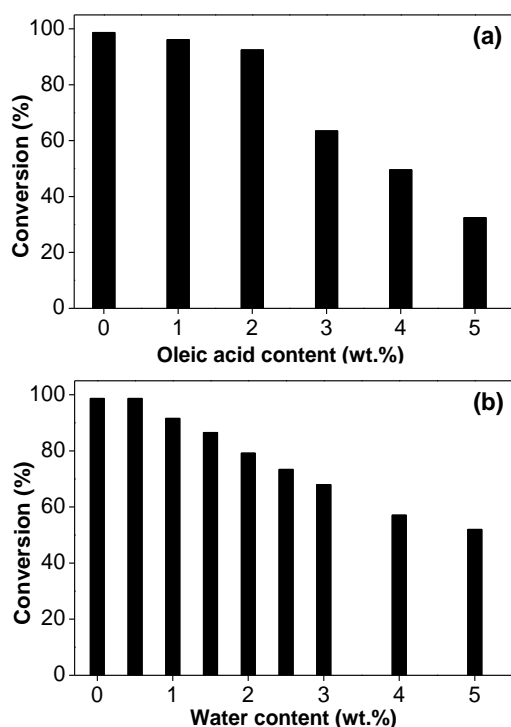


Fig. 4. Effect of (a) oleic acid and (b) water content on the transesterification. Reaction conditions: feedstock-to-methanol molar ratio (1 : 20), catalyst loading (6 wt.%), reaction temperature (120 °C) and reaction time (1 h).

Further investigation on the FFA tolerance of the Ca/Fe catalytic system was studied as illustrated in Fig. 4a. The

refined food grade canola oil and oleic acid were used as model feedstock and FFA respectively in this study. A series of stimulated feedstock samples with different amount of oleic acid (Table S2 in supplementary section) mixed with refined food canola oil were used for one-step simultaneous esterification and transesterification. It was found that the catalyst tolerated oleic acid of 2.00 wt.% with a remarkable conversion at 92.5 %. The Ca/Fe catalytic system demonstrated a high robustness towards highly FFA contaminated feedstock. The $\text{Ca}_2\text{Fe}_2\text{O}_5$ showed much higher FFA tolerance than that of the NaOH in which the NaOH system would induce saponification with a higher FFA content (>1 wt.%).^{28, 57} For comparison, the same reaction using corresponding amount of CaO was also tested. It was found that CaO could still catalyze the transesterification but it was totally dissolved at the end of the reaction which pointed out that CaO did undergo homogeneous catalysis rather than heterogeneous catalysis.

3.7 Study of water tolerance

The water tolerance of the Ca/Fe catalytic system was examined as depicted in Fig. 4b. A series of stimulated feedstock samples containing different amount of water (Table S3 in supplementary section) mixed with refined food canola oil were used for catalytic transesterification. The catalyst could withstand water of 1.00 wt.% with a noteworthy conversion at 91.6 % in which the catalyst can even applied in low grade methanol. The Ca/Fe catalyst behaved a higher water tolerance than that of the existing homogeneous base catalyst. It is comparable to our previous work on sulfated zirconium oxide which showed even higher tolerance.^{58, 59}

Conclusions

A series of alkaline earth metal-transition metal catalytic systems were explored for transesterification with methanol. The Ca/Fe catalytic system, due to the stabilization of Fe, gave the highest catalytic stability and robustness towards refined and unrefined feedstock. Through the Taguchi analysis, the conversion was achieved at 99.5 % under optimal reaction conditions ANOVA test suggested the reaction temperature to be prominent factor which contributed 82.84 % to the overall conversion. The $\text{Ca}_2\text{Fe}_2\text{O}_5$ catalytic system was applied to one-step simultaneous esterification and transesterification and tolerated a feedstock containing a significant amount of FFA (2 wt.%) and water (1 wt.%).

Acknowledgements

The authors grateful acknowledge the financial support from The Hong Kong Research Grants Council, The Hong Kong Polytechnic University. T. L. Kwong acknowledges the receipt of postgraduate studentship administrated by The Hong Kong Polytechnic University.

Notes and references

- 1 F. Ma and M. A. Hanna, *Bioresour. Technol.*, 1999, **70**, 1-15.
- 2 A. Demirbas, *Prog. Energy Combust. Sci.*, 2005, **31**, 466-487.
- 3 R. Jothiramalingam and M. K. Wang, *Ind. Eng. Chem. Res.*, 2009, **48**, 6162-6172.
- 4 A. P. Vyas, J. L. Verma and N. Subrahmanyam, *Fuel*, 2010, **89**, 1-9.
- 5 J. M. Marchetti, V. U. Miguel and A. F. Errazu, *Renew. Sustain. Energy Rev.*, 2007, **11**, 1300-1311.
- 6 D. Lee, Y. Park and K. Lee, *Catal. Surv. Asia*, 2009, **13**, 63-77.
- 7 T. F. Dossin, M. Reyniers and G. B. Marin, *Appl. Catal. B: Environ.*, 2006, **62**, 35-45.
- 8 S. Gryglewicz, *Appl. Catal. A: Gen.*, 2000, **192**, 23-28.
- 9 S. Gryglewicz, *Bioresour. Technol.*, 1999, **70**, 249-253.
- 10 M. L. Granados, M. D. Z. Poves, D. M. Alonso, R. Mariscal, F. C. Galisteo, R. Moreno-Tost, J. Santamaría and J. L. G. Fierro, *Appl. Catal. B: Environ.*, 2007, **73**, 317-326.
- 11 E. S. Umdu and E. Seker, *Bioresour. Technol.*, 2012, **106**, 178-181.
- 12 G. Pacchioni, J. M. Ricart and F. Illas, *J. Am. Chem. Soc.*, 1994, **116**, 10152-10158.
- 13 S. Yan, H. Lu and B. Liang, *Energy Fuels*, 2008, **22**, 646-651.
- 14 M. Kouzu, S. Yamanaka, J. Hidaka and M. Tsunomori, *Appl. Catal. A: Gen.*, 2009, **355**, 94-99.
- 15 A. K. Singh and S. D. Fernando, *Energy Fuels*, 2008, **22**, 2067-2069.
- 16 M. L. Granados, D. M. Alonso, I. Sádaba, R. Mariscal and P. Ocón, *Appl. Catal. B: Environ.*, 2009, **89**, 265-272.
- 17 H. Mootabadi, B. Salamatinia, S. Bhatia and A. Z. Abdullah, *Fuel*, 2010, **89**, 1818-1825.
- 18 J. Jitputti, B. Kitiyanan, P. Rangsunvigit, K. Bunyakiat, L. Attanatho and P. Jenvanitpanjakul, *Chem. Eng. J.*, 2006, **116**, 61-66.
- 19 H. Kim, B. Kang, M. Kim, Y. M. Park, D. Kim, J. Lee and K. Lee, *Catal. Today*, 2004, **93-95**, 315-320.
- 20 W. Xie, H. Peng and L. Chen, *Appl. Catal. A: Gen.*, 2006, **300**, 67-74.
- 21 M. C. G. Albuquerque, I. Jiménez-Urbistondo, J. Santamaría-González, J. M. Mérida-Robles, R. Moreno-Tost, E. Rodríguez-Castellón, A. Jiménez-López, D. C. S. Azevedo, C. L. Cavalcante Jr. and P. Maireles-Torres, *Appl. Catal. A: Gen.*, 2008, **334**, 35-43.
- 22 J. M. Rubio-Caballero, J. Santamaría-González, J. Mérida-Robles, R. Moreno-Tost, A. Jiménez-López and P. Maireles-Torres, *Appl. Catal. B: Environ.*, 2009, **91**, 339-346.
- 23 A. C. Alba-Rubio, J. Santamaría-González, J. M. Mérida-Robles, R. Moreno-Tost, D. Martín-Alonso, A. Jiménez-López and P. Maireles-Torres, *Catal. Today*, 2010, **149**, 281-287.
- 24 D. G. Cantrell, L. J. Gillie, A. F. Lee and K. Wilson, *Appl. Catal. A: Gen.*, 2005, **287**, 183-190.
- 25 S. Yan, M. Kim, S. Mohan, S. O. Salley and K. Y. S. Ng, *Appl. Catal. A: Gen.*, 2010, **373**, 104-111.
- 26 L. F. Man, W. T. Wong and K. F. Yung, *J. Clust. Sci.*, 2012, **23**, 873-884.
- 27 G. Guan, K. Kusakabe, N. Sakurai and K. Moriyama, *Fuel*, 2009, **88**, 81-86.
- 28 H. J. Berchmans and S. Hirata, *Bioresour. Technol.*, 2008, **99**, 1716-1721.
- 29 D. Hirabayashi, T. Yoshikawa, K. Mochizuki, K. Suzuki and Y. Sakai, *Catal. Letters*, 2006, **110**, 155-160.
- 30 B. Xue, J. Luo, F. Zhang and Z. Fang, *Energy*, 2014, **68**, 584-591.
- 31 C. Chuanwen, S. Feng, L. Yuguo and W. Shuyun, *J. Mater. Sci.: Mater. Electron.*, 2010, **21**, 349-354.
- 32 S. G. Hosseini and A. Eslami, *Prog. Org. Coat.*, 2010, **68**, 313-318.
- 33 X. Wu and D. Y. C. Leung, *Appl. Energy*, 2011, **88**, 3615-3624.
- 34 Y. Yamini, N. Bahramifar, F. Sefidkon, M. J. Saharkhiz and E. Salamifar, *Nat. Prod. Res.*, 2008, **22**, 212-218.
- 35 S. M. Pourmortazavi, S. S. Hajimirsadeghi, I. Kohsari, R. Fareghi Alamdari and M. Rahimi-Nasrabadi, *Chem. Eng. Technol.*, 2008, **31**, 1532-1535.
- 36 C. Samart, C. Chaia and P. Reubroycharoen, *Energy Convers. Manag.*, 2010, **51**, 1428-1431.
- 37 G. Knothe, *J. Am. Oil Chem. Soc.*, 2000, **77**, 489-493.
- 38 G. F. Ghesti, J. L. de Macedo, I. S. Resck, J. A. Dias and S. Dias, *Energy Fuels*, 2007, **21**, 2475-2480.
- 39 J. K. Satyarthi, D. Srinivas and P. Ratnasamy, *Energy Fuels*, 2009, **23**, 2273-2277.
- 40 J. V. Gerpen, *Fuel Process. Technol.*, 2005, **86**, 1097-1107.
- 41 H. Hoydonckx, D. De Vos, S. Chavan and P. Jacobs, *Top. Catal.*, 2004, **27**, 83-96.
- 42 A. Kawashima, K. Matsubara and K. Honda, *Bioresour. Technol.*, 2008, **99**, 3439-3443.
- 43 P. Zhang, Q. Han, M. Fan and P. Jiang, *Appl. Surf. Sci.*, 2014, **317**, 1125-1130.
- 44 G. Teng, L. Gao, G. Xiao and H. Liu, *Energy Fuels*, 2009, **23**, 4630-4634.
- 45 N. Viriya-empikul, P. Krasae, W. Nualpaeng, B. Yoosuk and K. Faungnawakij, *Fuel*, 2012, **92**, 239-244.
- 46 Y. Li, S. Lian, D. Tong, R. Song, W. Yang, Y. Fan, R. Qing and C. Hu, *Appl. Energy*, 2011, **88**, 3313-3317.
- 47 E. Lotero, Y. Liu, D. E. Lopez, K. Suwannakarn, D. A. Bruce and J. G. Goodwin, *Ind. Eng. Chem. Res.*, 2005, **44**, 5353-5363.
- 48 H. Zeng, Z. Feng, X. Deng and Y. Li, *Fuel*, 2008, **87**, 3071-3076.
- 49 W. Xie, H. Peng and L. Chen, *J. Mol. Catal. A: Chem.*, 2006, **246**, 24-32.
- 50 Q. Shu, J. Gao, Z. Nawaz, Y. Liao, D. Wang and J. Wang, *Appl. Energy*, 2010, **87**, 2589-2596.
- 51 D. Rattanaphra, A. Harvey and P. Srinophakun, *Top. Catal.*, 2010, **53**, 773-782.
- 52 E. Li, Z. P. Xu and V. Rudolph, *Applied Catalysis B: Environmental*, 2009, **88**, 42-49.
- 53 D. Kusdiana and S. Saka, *Fuel*, 2001, **80**, 693-698.
- 54 P. S. Sreeprasanth, R. Srivastava, D. Srinivas and P. Ratnasamy, *Applied Catalysis A: General*, 2006, **314**, 148-159.
- 55 J. Park, D. Kim and J. Lee, *Bioresour. Technol.*, 2010, **101**, S62-S65.
- 56 M. G. Kulkarni and A. K. Dalai, *Ind. Eng. Chem. Res.*, 2006, **45**, 2901-2913.
- 57 E. Crabbe, C. Nolasco-Hipolito, G. Kobayashi, K. Sonomoto and A. Ishizaki, *Process Biochem.*, 2001, **37**, 65-71.
- 58 Y. Zhang, W. T. Wong and K. F. Yung, *Appl. Energy*, 2014, **116**, 191-198.
- 59 Y. Zhang, W. T. Wong and K. F. Yung, *Bioresour. Technol.*, 2013, **147**, 59-64.